Journal of Anatomy

J. Anat. (2012) **221**, pp128–137 doi: 10.1111/j.1469-7580.2012.01519.x

Ontogeny of the cranial system in *Laonastes aenigmamus*

Anthony Herrel,[1] Anne-Claire Fabre,[2–4] Jean-Pierre Hugot,[5] Kham Keovichit,[6] Dominique Adriaens,[7] Loes Brabant,[8] Luc Van Hoorebeke[8] and Raphael Cornette[5,9]

[1]*UMR CNRS/MNHN 7179, Mécanismes adaptatifs: des organismes aux communautés, Paris, France*
[2]*Centre de Recherches sur la Paléobiodiversité et les paléoenvironnements, UMR 7207 CNRS MNHN, Paris, France*
[3]*Université Paris Diderot, Paris, France*
[4]*Department of Genetics, Evolution and Environment, and Department of Earth Sciences, University College London, London, UK*
[5]*UMR CNRS/MNHN 7205, Origine, Structure et Evolution de la Biodiversité, Muséum National d'Histoire Naturelle, Paris, France*
[6]*National Agriculture and Forestry Research Institute (NAFRI), Vientiane, Lao PDR*
[7]*Ghent University, Evolutionary Morphology of Vertebrates, Gent, Belgium*
[8]*UGCT, Department of Physics and Astronomy, Ghent University, Gent, Belgium*
[9]*UMS CNRS/MNHN 2700, Outils et Méthodes de la Systématique Intégrative, Plate-forme de morphométrie, Paris, France*

Abstract

Rodents, together with bats, are among the ecologically most diverse and most speciose groups of mammals. Moreover, rodents show elaborate specializations of the feeding apparatus in response to the predominantly fore-aft movements of the lower jaw. The Laotian rock rat *Laonastes aenigmamus* was recently discovered and originally thought to belong to a new family. The difficulties in classifying *L. aenigmamus* based on morphological characters stem from the fact that it presents a mixture of sciurognathous and hystricognathous characteristics, including the morphology of the jaw adductors. The origin of the unusual muscular organization in this species remains, however, unclear. Here, we investigate the development of the masticatory system in *Laonastes* to better understand the origin of its derived morphology relative to other rodents. Our analyses show that skull and mandible development is characterized by an overall elongation of the snout region. Muscle mass increases with positive allometry during development and growth, and so does the force-generating capacity of the jaw adductor muscles (i.e. physiological cross-sectional area). Whereas fetal crania and musculature are more similar to those of typical rodents, adults diverge in the elongation of the rostral part of the skull and the disproportionate development of the zygomaticomandibularis. Our data suggest a functional signal in the development of the unusual cranial morphology, possibly associated with the folivorous trophic ecology of the species.
Key words: feeding; jaw muscle; mammal; ontogeny; scaling; skull.

Introduction

Rodents, together with bats, are among the ecologically most diverse and most speciose groups of mammals (Wilson & Reeder, 2005). Moreover, rodents show one of the most extreme specializations of the feeding apparatus, with a single pair of highly specialized upper and lower incisors used for gnawing, and a small number of cheek teeth used for chewing. These specializations are associated with a specialized musculature (Schumacher, 1961) facilitating the antero-posterior jaw movements typical of rodents (propaliny; see Becht, 1953). The exceptional diversity of rodents is, moreover, associated with a diverse array of specializations of the jaw musculature (Weijs, 1973; Woods & Hermanson, 1985; Offermans & De Vree, 1989; Druzinsky, 2010a,b; Cox & Jeffery, 2011; Hautier et al. 2011a). Variations in the masseter complex, and the associated modifications of the skull, have traditionally been used as diagnostic characters to classify rodents (Hautier et al. 2011a).

The Laotian rock rat *Laonastes aenigmamus* was recently discovered in the Lao People's Democratic Republic (Jenkins et al. 2005). Although this species was originally thought to belong to a new family, a reexamination of the specimen

Correspondence
Anthony Herrel, UMR 7179 C.N.R.S/M.N.H.N., Département d'Ecologie et de Gestion de la Biodiversité, 55 rue Buffon, CP 55, 75005 Paris, France. T: ++33 140798120; F: ++33 140793773; E: anthony.herrel@mnhn.fr

Accepted for publication *25 April 2012*
Article published online *21 May 2012*

Table 1 Body and cranial dimensions of the individuals dissected in this study.

Individual	Sex	Body length (mm)	Skull length (mm)	Skull width (mm)	Skull depth (mm)	Use
KY161	F	255	66.91	26.85	24.76	D
KY180	F	175	56.80	24.23	20.59	D, MO
KY132	M	231	62.35	25.71	23.73	D
KY211	M	248	66.73	27.6	24.34	D, MO
KY213	F	237	65.28	26.35	23.77	D, MO
KY167	M	245	62.32	25.15	16.92	MO
KY186	M	257	67.52	27.12	18.05	MO
KY110	M	277	56.39	24.65	16.04	MO
KY038	F	255	56.57	24.33	16.29	MO
KY$	J	234	58.17	23.90	16.59	MO
KY087	Fetus	67.55	28.98	16.89	14.53	D, MO
KY080	Fetus*					MO

Table entries include measurements taken on the preserved specimens.
D, dissection; F, female; J, unsexed juvenile; M, male; MO, morphometrics.
*Scanned inside uterus, no dimensions available.

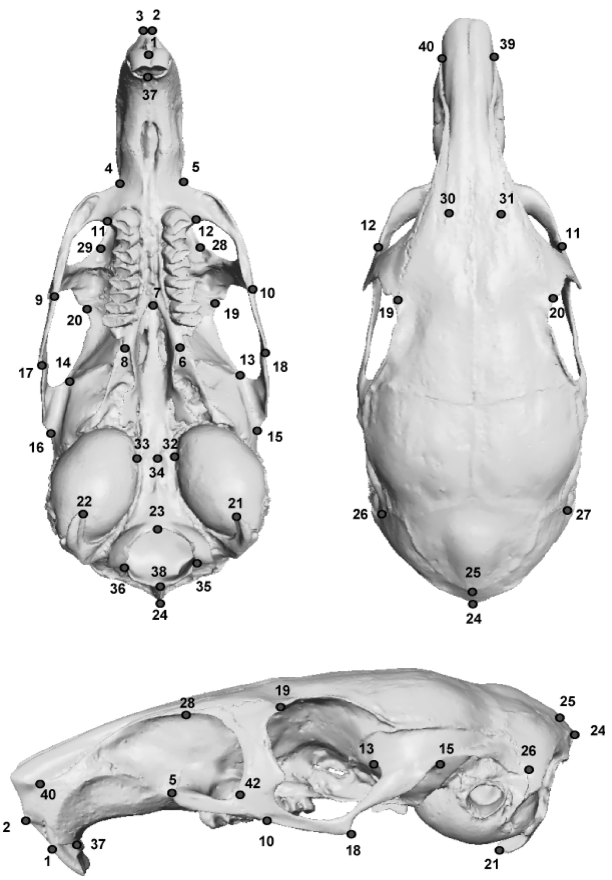

Fig. 1 Figure illustrating the landmarks used to quantify ontogenetic variation in the skull. Illustrated are a lateral (bottom), ventral (top left) and dorsal view of the skull. See Table 2 for landmark definitions.

(Dawson et al. 2006) showed that it belongs to the otherwise extinct family Diatomyidae. Moreover, recent molecular analyses confirmed the placement of *L. aenigmamus* as a sister taxon to the Ctenodactylidae (Huchon et al. 2007). The difficulties in classifying *L. aenigmamus* using morphological characters stem from the fact that it presents a mixture of sciurognathous and hystricognathous characteristics (Jenkins et al. 2005; Dawson et al. 2006; Huchon et al. 2007). Indeed, a recent analysis of the anatomy of adult *Laonastes* demonstrated that the pars reflexa of the masseter complex in *Laonastes* has evolved independently in this species (Hautier & Saksiri, 2009). This suggests that the masseter complexity contains a functional rather than a phylogenetic signal, and that variation in the jaw adductors may be tuned to functional demands. However, the origin of the unusual muscular organization in this species remains unclear given that all of its closest relatives are extinct. Here, we propose to investigate the development of the masticatory system in *Laonastes* to better understand the origin of its derived morphology and potential functional specializations relative to other rodents.

Although developmental data may provide profound insights into the origin and homology of derived anatomical patterns, relatively few studies have investigated the ontogeny of the cranial system in mammals in general, and rodents in particular. Indeed, despite a recent revival of

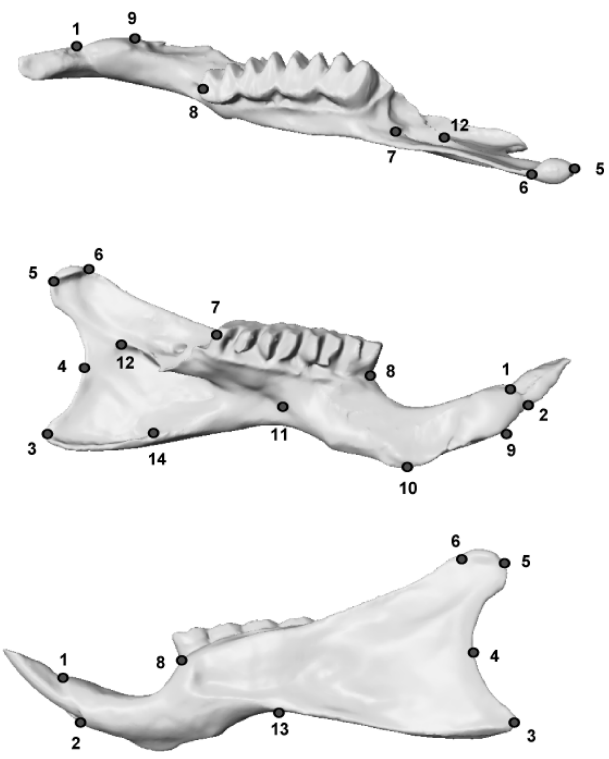

Fig. 2 Figure illustrating the landmarks used to quantify ontogenetic variation in the mandible. Illustrated are a dorsal (top), lingual (middle) and lateral view of the mandible. See Table 2 for landmark definitions.

Table 2 Definitions of the landmarks used for geometric morphometrics.

Cranium	
1	Most anterior point where the premaxillar suture meets the anterior part of alveolar margin of the incisives, midline
2	Most antero-dorsal point of the premaxillar suture, left side
3	Most antero-dorsal point of the premaxillar suture, right side
4	Most anterior point of the infra-orbital canal, right side
5	Most anterior point of the infra-orbital canal, left side
6	Most anterior point of the pterygoid apophysis that meets the alisphenoid, left side
7	Most anterior point of the palatine suture, midline
8	Most anterior point of the pterygoid apophysis that meets the alisphenoid, right side
9	Most ventral point jugal/maxilla suture, right side
10	Most ventral point jugal/maxilla suture, left side
11	Most posterior point of insertion of the maxilla part of the zygomatic arch to the tooth row, right side
12	Most posterior point of insertion of the maxilla part of the zygomatic arch to the tooth row, left side
13	Most anterior point of insertion of the squamosal part of the zygomatic arch to the cephalic capsule, left side
14	Most anterior point of insertion of the squamosal part of the zygomatic arch to the cephalic capsule, right side
15	Most posterior point of insertion of the squamosal part of the zygomatic arch to the cephalic capsule, left side
16	Most posterior point of insertion of the squamosal part of the zygomatic arch to the cephalic capsule, right side
17	Most posterior point of the zygomatic arch (jugal), right side
18	Most posterior point of the zygomatic arch (jugal), left side
19	Point of frontal/lacrymal suture, left side
20	Point of frontal/lacrymal suture, right side
21	Tip of the paroccipital apophysis, left side
22	Tip of the paroccipital apophysis, right side
23	Most antero-ventral point of the foramen magnum, midline
24	Most postero-ventral point of the occipital crest, midline
25	Most posterior point of the interparietal, midline
26	Most lateral point of the exooccipital/parietal/squamosal suture, left side
27	Most lateral point of the exooccipital/parietal/squamosal suture, right side
28	Most antero-dorsal point of insertion of the zygomatic arch to the snout, left side
29	Most antero-dorsal point of insertion of the zygomatic arch to the snout, right side
30	Most posterior point of maxilla/nasal/frontal, left side
31	Most posterior point of maxilla/nasal/frontal, right side
32	Most antero-lateral point of the basioccipital that meets the basisphenoid and the tympanic bulla, left side
33	Most antero-lateral point of the basioccipital that meets the basisphenoid and the tympanic bulla, right side
34	Most antero-central point of the basioccipital/basisphenoid suture, midline
35	Most lateral point of foramen magnum, left side
36	Most lateral point of foramen magnum, right side
37	Most posterior point where the premaxillar suture meets the posterior part of alveolar margin of the incisives, midline
38	Most postero-dorsal point of the foramen magnum, midline
39	Most anterior point premaxilla/nasal suture, right side
40	Most anterior point premaxilla/nasal suture, left side
41	Most anterior point maxilla/jugal suture, right side
42	Most anterior point maxilla/jugal suture, left side
Mandible	
1	Most antero-dorsal point of the mandibular symphysis that meets the posterior part of the alveolar margin of the incisive
2	Most antero-ventral point of the mandibular symphysis that meets the anterior part of the alveolar margin of the incisive
3	Tip of the angular process
4	Point that is at the maximum of concavity between the condyloid and the angular process
5	Most posterior point of the edge of the articular surface condyle
6	Most anterior point of the edge of the articular surface condyle
7	Most posterior point of the alveolar margin of the premolar-molar row
8	Most anterior point of the alveolar margin of the premolar-molar row
9	Most postero-ventral point of symphysis of the left dentary
10	Point of maximum of convexity of the antero-ventral part of the dentary
11	Most ventral point of insertion of the molar row to the medial body of the mandible
12	Point of insertion of the medial dental ridge to the condyloid process
13	Point of maximum of concavity of the ventral margin of the mandible
14	Most anterior point of the groove of the medial part of the angular process

Numbers correspond to the landmark numbers as illustrated in Fig. 1.

developmental studies investigating the early development and patterning of the cranial musculature in mammals (Smith, 1994; Goswami, 2007; Sánchez-Villagra et al. 2008; Wilson & Sanchez-Villagra, 2009; Hautier et al. 2011b), almost nothing is known about the late development and postnatal growth of the cranial system (but see, e.g. Strong, 1926; De Beer, 1937; Hughes et al. 1978; Maier et al. 2003; Flores et al. 2010), and even less about the development of the associated musculature. From a functional perspective, however, such studies can provide profound insights into the selective patterns operating during early ontogeny, which ultimately determine the adult form of an organism (e.g. Herrel et al. 2005; Wyckmans et al. 2007; Herrel & Holanova, 2008; Genbrugge et al. 2011) and may help

Table 3 Results of regressions of muscle data vs. cranial length.

Muscle	Slope ± SE	Intercept	r^2	*P*
Mass (g)				
M. temporalis**	4.22 ± 0.29	−9.08	0.98	< 0.001
M. temporalis pars orbitalis	3.92 ± 0.47	−8.82	0.95	0.001
M. temporalis pars posterior	3.62 ± 0.30	−8.27	0.97	< 0.001
M. masseter superficialis pars anterior*	4.42 ± 0.51	−9.16	0.95	0.001
M. masseter superficialis pars reflexa**	4.91 ± 0.17	−9.38	0.99	< 0.001
M. masseter lateralis pars anterior	4.36 ± 0.74	−8.90	0.90	0.004
M. masseter lateralis pars posterior**	4.93 ± 0.33	−9.72	0.98	< 0.001
M. masseter posterior**	3.90 ± 0.34	−8.67	0.97	< 0.001
M. masseter pars infraorbitalis**	4.49 ± 0.40	−8.77	0.97	< 0.001
M. masseter pars zygomatica**	5.75 ± 0.26	−11.09	0.99	< 0.001
M. pterygoideus pars internus**	4.76 ± 0.19	−9.34	0.99	< 0.001
M. pterygoideus pars externus**	4.22 ± 0.23	−8.68	0.99	< 0.001
M. digastricus**	3.85 ± 0.12	−7.99	0.99	< 0.001
Fiber length (mm)				
M. temporalis*	1.34 ± 0.10	−1.52	0.98	< 0.001
M. temporalis pars orbitalis	1.21 ± 0.23	−1.45	0.88	0.006
M. temporalis pars posterior	0.98 ± 0.54	−0.94	0.45	NS
M. masseter superficialis pars anterior	1.42 ± 0.25	−1.64	0.89	0.005
M. masseter superficialis pars reflexa	1.15 ± 0.21	−1.16	0.89	0.005
M. masseter lateralis pars anterior	0.99 ± 0.15	−0.92	0.92	0.002
M. masseter lateralis pars posterior	1.22 ± 0.19	−1.39	0.91	0.003
M. masseter posterior	1.48 ± 0.37	−1.93	0.80	0.02
M. masseter pars infraorbitalis	1.05 ± 0.36	−1.02	0.68	0.04
M. masseter pars zygomatica	0.98 ± 0.17	−0.91	0.90	0.004
M. pterygoideus pars internus	0.86 ± 0.23	−0.83	0.78	0.02
M. pterygoideus pars externus	0.55 ± 0.20	−0.27	0.65	0.05
M. digastricus	1.03 ± 0.13	−1.04	0.94	0.001
Physiological cross-sectional area (cm^2)				
M. temporalis*	2.88 ± 0.31	−6.53	0.96	0.001
M. temporalis pars orbitalis	2.71 ± 0.48	−6.35	0.89	0.005
M. temporalis pars posterior	2.64 ± 0.38	−6.31	0.92	0.002
M. masseter superficialis pars anterior	3.00 ± 0.60	−6.49	0.86	0.008
M. masseter superficialis pars reflexa**	3.75 ± 0.23	−7.20	0.99	< 0.001
M. masseter lateralis pars anterior	3.37 ± 0.61	−6.95	0.88	0.005
M. masseter lateralis pars posterior**	3.71 ± 0.45	−7.31	0.94	0.001
M. masseter posterior	2.42 ± 0.59	−5.70	0.81	0.02
M. masseter pars infraorbitalis	3.44 ± 0.60	−6.72	0.89	0.005
M. masseter pars zygomatica**	4.77 ± 0.22	−9.15	0.99	< 0.001
M. pterygoideus pars internus**	3.90 ± 0.23	−7.49	0.99	< 0.001
M. pterygoideus pars externus**	3.67 ± 0.39	−7.39	0.96	0.001
M. digastricus**	2.82 ± 0.19	−5.92	0.98	< 0.001

P represents *P*-value for the significance of a test evaluating whether the regression is different from 0.
*Indicates slopes significantly different from the slopes predicted by geometric scaling (i.e. 3 for mass, 1 for fiber length and 2 for physiological cross-sectional area) at $\alpha = 0.05$.
**Indicates significance at $\alpha = 0.01$.

understand the systematic position of taxa characterized by highly derived anatomical features (Maier et al. 2003). Here, we study ontogenetic changes in the shape of the cranium and mandible in the Laotian rock rat. Moreover, we explore whether the observed ontogenetic changes in skull shape are associated with ontogenetic changes in the jaw adductor musculature. Finally, functionally relevant aspects of the jaw adductor anatomy are compared with other rodents and interpreted in the context of what is known about the ecology of *Laonastes*.

Materials and methods

Specimen collection

The collection and use of *L. aenigmamus* has been regulated in Lao PDR since November 2008. Since January 2009 this species is listed as 'Endangered' on the IUCN Red List. For our study we obtained a research and collecting permit (letter of authorization N° 1183, 9 June 2008) from the Lao Government. The Khammuan Province Agriculture and Forestry Office (PAFO) validated our field collection schedule and an officer escorted us during collection trips. All animals used in this study were collected in Khammouane province and are deposited in the collections of the Muséum National d'Histoire Naturelle.

Specimens and scanning

Six individuals of formaldehyde-preserved specimens of *L. aenigmamus* including adults, juveniles and one fetus were used for dissection (skull length: 29–67 mm; Table 1). For comparative purposes two adult male *Rattus rattus* (skull length: 47.81 ± 0.16 mm) and two adult male *Cavia porcellus* (skull length: 56.55 ± 0.10 mm) were also dissected.

In addition, 10 specimens of *L. aenigmamus* of different ontogenetic stages (two fetuses at different stages of development but of unknown age, three juveniles and five adults) were included in our morphometric analysis. The two fetuses and three of the adults were scanned at the UGCT scanning facility at Ghent University (http://www.ugct.ugent.be) using a microfocus transmission-type X-ray tube. Depending on sample size, tube voltage was chosen between 80 and 100 kV, and an open type dual-head tube (Feinfocus FXE160.50 and FXE160.51) was used providing sufficiently small spot size. Specimens were mounted on a controllable rotating table (MICOS, UPR160F-AIR). For each specimen a series of 1000 projections of 1496 1880 pixels was recorded, covering 360. Reconstruction of the tomographic projection data was done using the in-house developed Octopus-package (Vlassenbroeck et al. 2007). Volume and surface rendering was performed using AVIZO 7.0 (VSG). The remainder of the specimens (cleaned skulls of three juveniles and two adults) was scanned using a surface scanner (stereoSCAN^{3D}; Breuckman GmbH, Meersburg, Germany) at the morphometrics platform of the Muséum National d'Histoire Naturelle.

Morphology

Specimens were measured using digital calipers (skull length, skull width and skull height; ± 0.01 mm Mitutoyo CD-15B), weighed and μCT scanned. Cranial muscles were removed under a binocular microscope (M5 Wild; Wild Heerbrugg, Gais, Switzerland). Muscles were removed on one side and transferred to labeled vials containing a 70% aqueous ethanol solution. Muscles were blotted dry and weighed to the nearest 0.01 mg using a microbalance (Mettler Toledo MT5; Mettler-Toledo, Columbus, OH, USA). Next, muscles were transferred to a 30% aqueous nitric acid solution and left for 24–28 h, after which the solution was replaced by a 50% aqueous glycerin solution. Individual fibers were teased apart using blunt-tipped glass needles, and 10–15 fibers were selected randomly and drawn using a binocular microscope with attached camera lucida (MT5 Wild). Drawings were scanned and fiber lengths determined using the ImageJ V1.31 software. Physiological cross-sectional areas were calculated by multiplying muscle mass by its density (1060 kg m^{-3}; Méndez & Keys, 1960) and dividing the thus calculated muscle volume by the average fiber length (Herrel et al. 2008). No correction for pennation angle was included as complex muscles were separated into their constituent parts defined by a single fiber orientation.

Morphometric analysis

Landmarks were always taken by the same person (A-CF) on the surface of 3D scans using the software package Idav Landmark

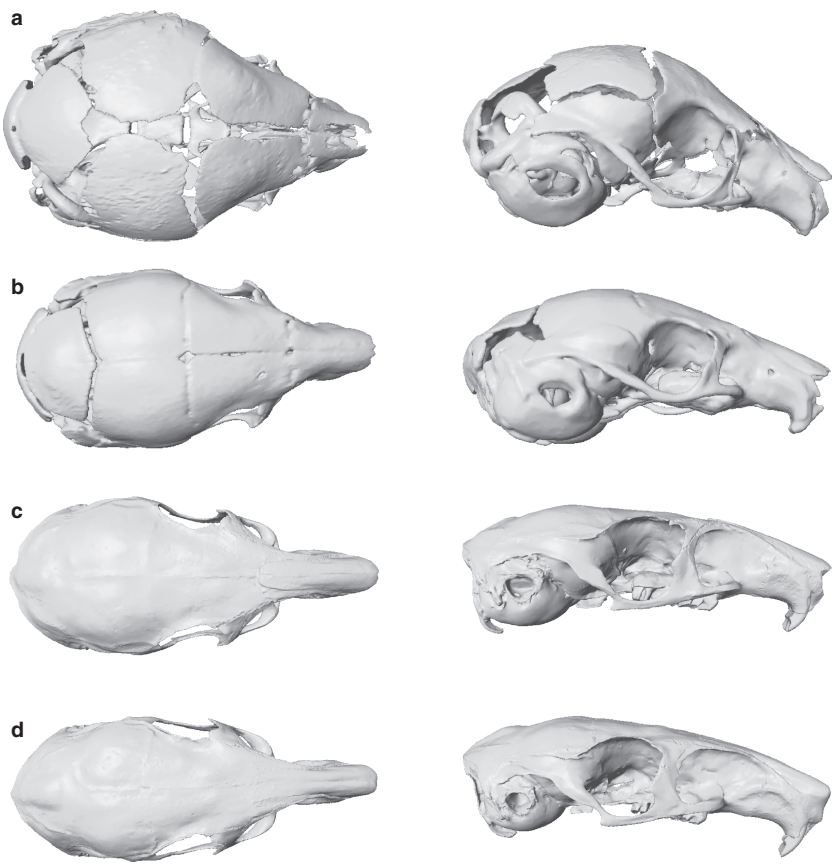

Fig. 3 Dorsal and lateral views of the skull of the two fetuses (a,b), a juvenile (c) and an adult (d) *Laonastes* illustrating the ossification of the skull and associated shape changes during late development and ontogeny. Note the late ossification of the skull roof and the narrowing and elongation of the skull and snout region.

(Wiley et al. 2005). Forty-two anatomical landmarks for the crania and 14 landmarks for the left mandible accurately describing the complex shape of the skull and mandible were chosen (Figs 1 and 2; Table 2 for definitions of landmarks). Note that we did not use the coronoid process as a landmark in our analysis of lower jaw shape due to the absence of a marked coronoid process in *Laonastes*. Two repetitions were done for each individual in order to assess measurement error, which was found to be low. Shape variation of the skull and mandible was assessed using geometric morphometric approaches allowing an analysis of size and shape components independently (Zelditch, 2004). Generalized Procrustes superimposition (Rohlf & Slice, 1990) was performed on the point coordinates using the package Rmorph (Baylac, 2012) in the program R (R Development Core Team, 2010). The Evan toolbox (http://www.evan.at) was used to perform a principal component analysis (PCA) and a visualization of shape variation along each axis using thin-plate splines in three dimensions. These visualizations were obtained by warping the consensus surface to the extremes of the PCA axes by minimizing the bending energy (Gunz et al. 2005).

Statistical analyses

All data were Log_{10}-transformed before analysis. To explore scaling relationships and growth of the masticatory muscles in *Laonastes*, we regressed the mass, fiber length and physiological cross-sectional area of each muscle against cranial length (Table 3). To test whether slopes differed from predictions of geometric growth (slope of 1 for length vs. length, 2 for area vs. length, and 3 for mass vs. length) we used a two-tailed *t*-test (Table 3).

Results

Skull development and growth

Overall skull development in *Laonastes* is typical of rodents (Strong, 1926) and characterized by an initial fusion of the cranial vault bones along the midline (Fig. 3a,b). Subsequently, the parietals fuse with the frontals. Fusion of the occipitals with the parietals takes place later in development, which is atypical for hystricognath rodents (Wilson & Sanchez-Villagra, 2009). Postnatal growth of the skull involves the increase of the cranial ridges that serve as insertion areas for the jaw adductor muscles and a continued growth of the facial region (Fig. 3c,d).

Morphometrics

Our analyses of cranial and mandibular shape indicate significant shape changes during growth (Figs 3–5). A PCA performed on the shape data extracted two axes that together describe over 75% of the variation in the data set for the cranium and over 64% of the overall variation in the mandible (Fig. 4). For both the cranium and the mandible, the first axis distinguishes between fetal specimens vs. juveniles and adults. The second axis discriminates between the fetuses and juveniles vs. adults. This suggests that most of the variation is driven by shape changes during early development (Fig. 3a–c). Figure 3 illustrates the shape changes in the cranium, and shows how during early development shape changes in the skull are characterized by a narrowing of the brain case and an elongation of the snout and the orbital region. The second axis indicates shape changes from juveniles to adults (Fig. 4), and is driven by a further narrowing of the brain case, a widening of the zygomatic arches, an elongation of the orbital region and a further elongation of the snout (Fig. 5a). Interestingly, shape changes in the snout region are exacerbated in the insertion area of the infraorbital part of the m. masseter

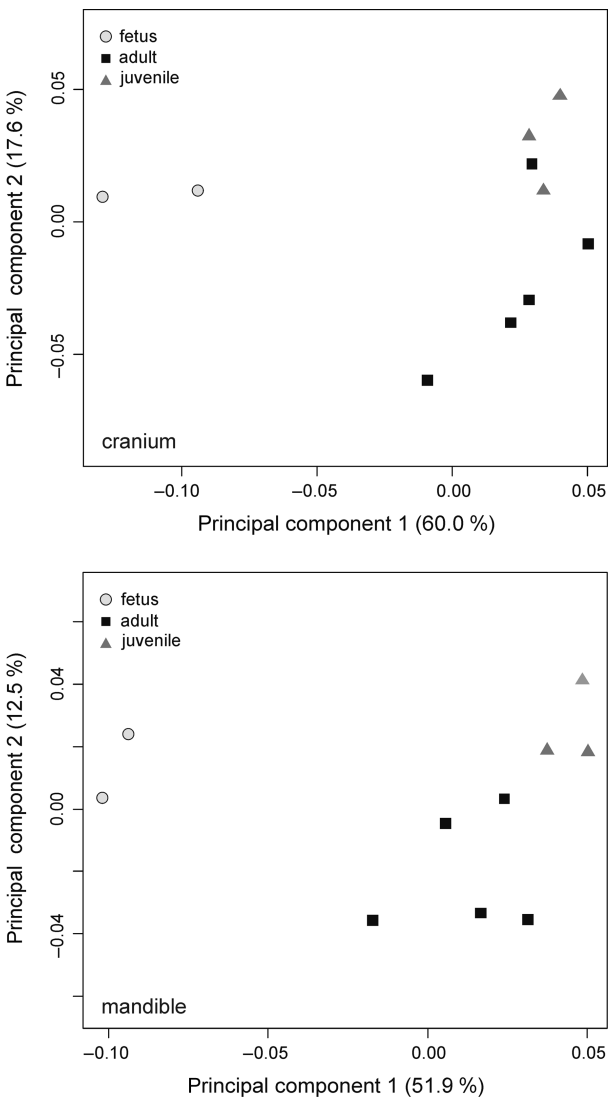

Fig. 4 Results of a PCA performed on the morphometric data for the skull (top) and mandible (bottom) of *Laonastes*. The first axis, which explains over 50% of the variation in the data set, clearly separates the pre- from the postnatal specimens for both the cranium and mandible. The second axis, which explains between 10 and 20% of the variance, contrasts the juvenile with the adult specimens. Gray circles: fetuses; dark gray triangles, juveniles; black squares, adults.

(Fig. 5a). With respect to the mandible, the first axis describing the shape change from fetal to adult specimens is characterized by a forward displacement of the jaw articulation relative to the angular process, a decrease in the height of the body of the mandible, an elongation of the diastema and a narrowing of the tooth row (Fig. 5b). The second axis, characterizing shape changes taking place from juveniles to adults, is characterized mostly by an increase of the curvature and a decrease in depth of the diastema. Overall, the lower jaw in adults is more slender, has a longer diastema, yet a larger insertion area for the internal pterygoid and the pars reflexa of the masseter.

Muscle anatomy and scaling

Here we follow the terminology and subdivisions of the adductor musculature as described by Hautier & Saksiri (2009). The overall anatomy of the jaw adductor musculature in *Laonastes* was similar to that described previously (Hautier & Saksiri, 2009). The scaling of the jaw muscles follows allometric patterns of growth, with all muscles except the m. temporalis pars orbitalis and the m. temporalis pars posterior showing positive allometry (Table 3; Fig. 6). Fiber lengths, on the other hand, showed mostly isometric growth, with the exception of the fibers of the main part of the m. temporalis where fibers get relatively longer as skulls get bigger (Table 3). As a consequence, the physiological cross-sectional areas of most muscles increased with positive allometry, indicating that the jaw adductors in adults have a greater force-generating capacity relative to body size than in fetal and juvenile animals (Table 3; Fig. 6).

Discussion

Our data show distinct shape changes in the cranium and mandible of *Laonastes* during development and growth. From a more general rodent-like shape, the rostral part of the cranium elongates, while the mandible shape changes to become more slender and with a more posteriorly positioned angular process. These shape changes appear to coincide with ontogenetic changes in muscle development, with jaw adductor muscles (notably the masseter complex) becoming heavier and disproportionately stronger in adults. These results are in contrast to data on the scaling of functionally important elements of the locomotor system, with juveniles often showing a more advanced development and function of the musculoskeletal system relative to adults (Carrier, 1983, 1995, 1996; Herrel & Gibb, 2006). Our data suggest that cranial development and growth in *Laonastes* is more similar to carnivores, which show a late maturation of cranial form and performance (e.g. Tanner et al. 2010; La Croix et al. 2011). However, in contrast to carnivores such as

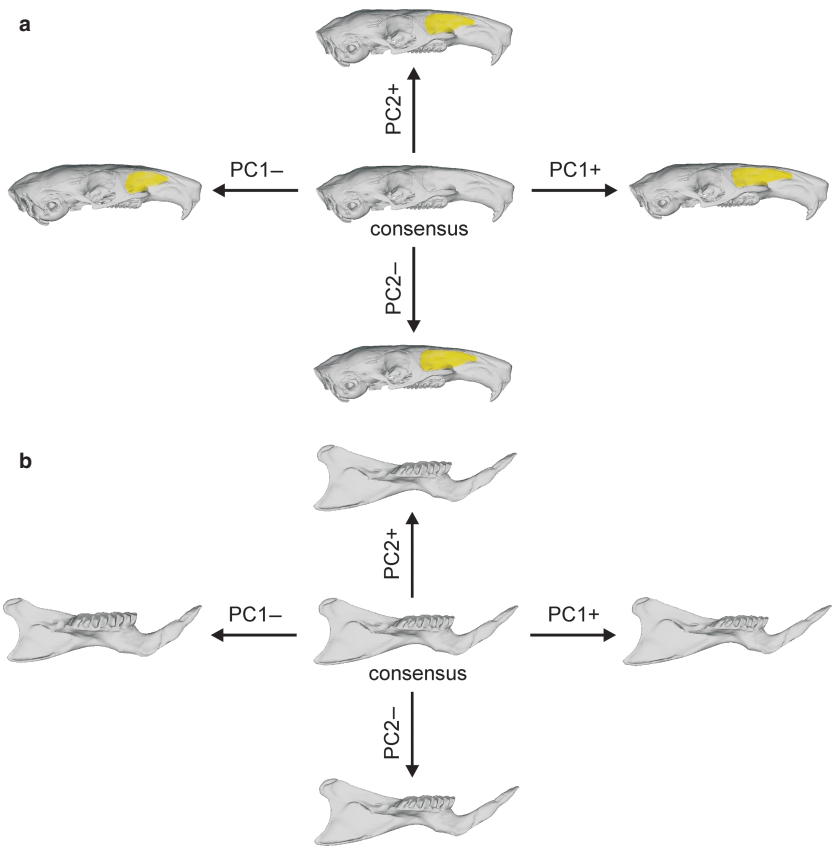

Fig. 5 Shape changes observed in the skull during ontogeny illustrated for the skull in lateral view. Whereas the fetus is characterized by a shorter snout and shallower back of the skull, adults have an elongated rostrum. Note how the insertion area of the infraorbital part of the masseter muscle (in yellow) is particularly affected by shape changes taking place during ontogeny.

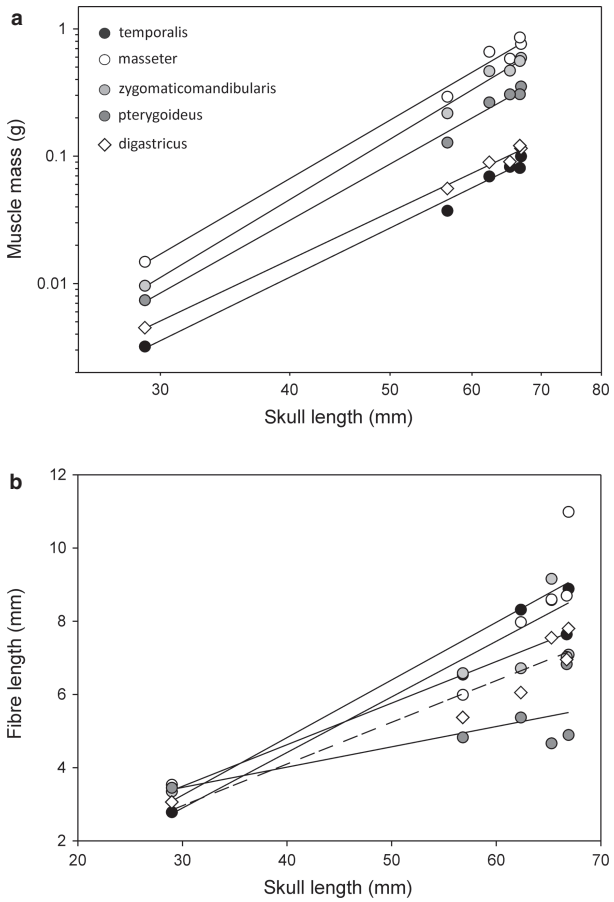

Fig. 6 Graphs illustrating the scaling of muscle mass (a) and fiber length (b) relative to cranial length in *Laonastes aenigmamus*. Different muscle groups are indicated by different colored symbols. Note the log-scale in (a) and the allometric scaling of muscle mass with skull length. Fiber lengths of different muscles scale differently with skull length, resulting in a disproportionately large physiological cross-sectional area of the zygomaticomandibularis in adult *Laonastes*, which corresponds to the observed changes in skull shape characterized by an elongation of the snout at the level of the insertion of this muscle.

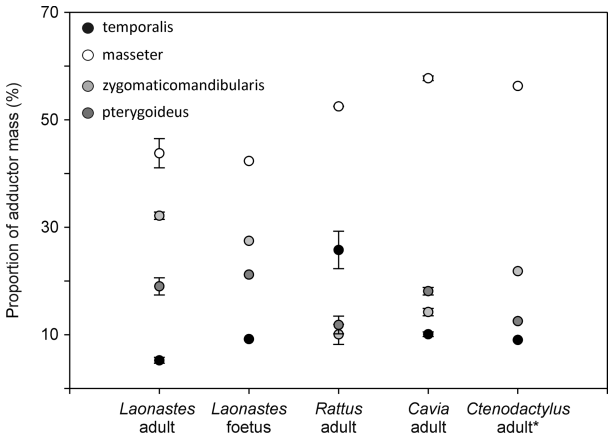

Fig. 7 Allocation of the jaw adductor musculature to different functional groups. Illustrated are the proportions of the different muscle groups relative to total jaw adductor mass for adult and fetal *Laonastes*, as well as for a rat and a guinea pig. Different colored symbols illustrate means ± SEM for the different muscle groups. Whereas fetal *Laonastes* are more similar to other rodents, adult *Laonastes* are characterized by an exceptionally large zygomaticomandibularis muscle group. *Data for *Ctenodactylus vali* (from Hautier, 2010).

Hyenas (Tanner et al. 2010), *Laonastes* shows an elongation of the rostrum with size, and an increase in the insertion area for the masseter rather than the temporalis. Although the specific increase in the insertion area of the masseter during growth is undoubtedly related to the masseteric dominance among the jaw adductors of rodents (Schumacher, 1961), the elongated rostrum may be related to the folivorous feeding habits of *Laonastes* (Scopin et al. 2011).

Indeed, a comparison of the allocation of the jaw adductor mass to the different functional groups shows that as adults *Laonastes* are divergent from rodents such as rats or guinea pigs (Fig. 7). Whereas the masseter sensu stricto is the biggest muscle in all rodents, in adult *Laonastes* the zygomaticomandibularis comprises 30% of the total jaw adductor mass in contrast to the 10–15% observed in rats and guinea pigs (Fig. 7). However, qualitative descriptions of the jaw adductors in members of the New World genus *Proechimys* suggest that these may have similar muscle allocation patterns (Woods, 1972; Hautier & Saksiri, 2009). Moreover, *Ctenodactylus vali* (Hautier, 2010; Fig. 7) also shows a disproportionate development of the zygomaticomandibularis muscle relative to rats or guinea pigs. Interestingly, the fetal *Laonastes* specimen dissected in this study shows a muscle allocation that is more similar to that observed in other rodents, with a relatively larger temporalis and smaller zygomaticomandibularis muscle. Yet, the coronoid process never develops as suggested by our fetal specimens.

These observations suggest that the unusual anatomy of *Laonastes* is likely related to aspects of its life-history and the use of the feeding system as adults. Previous examinations of the digestive tract anatomy of *Laonastes* have suggested that the digestive system may be specialized for folivory, a trait unusual for rodents. Indeed, even compared with the closely related gundis (*Ctenodactylus*), *Laonastes* has an exceptionally long rostrum and extensive development of the infraorbital part of the masseter muscle (Hautier & Saksiri, 2009; Hautier, 2010). From a functional perspective, the elongation of the snout and anterior insertion of the infraorbital part of the masseter likely provides a greater horizontal force component upon contraction, which will result in a more extensive anteriad displacement of the lower jaw during jaw closure. Moreover, the strong development of the masseter complex relative to the temporalis and the rather horizontal position of the temporalis indicate an optimal functioning of the

jaw system at very low gape angles, which would accord well with the suggested folivorous feeding habit (Wright et al. 2008). The relatively strong development of the anterior portion of the masseter also assures a uniform force generation across the entire tooth row, which may be beneficial in reducing fibrous plant material such as leaves (Onoda et al. 2011). Adaptive hypotheses regarding the specialization of the masticatory system in the function of a folivorous diet could be tested by careful biomechanical modeling of representative rodents with different feeding ecologies.

Acknowledgements

We would like to thank Phil Cox and Lionel Hautier for stimulating discussions on rodent cranial anatomy and function, and both Lionel Hautier and Sharlene Santana for constructive and helpful comments on a previous version of this paper. Lionel Hautier also kindly provided data on muscle mass allocation in *Ctenodactylus vali*. A-CF would like to thank the Ecole doctorale interdisciplinaire Européene Frontières du vivant ED474 program doctoral Liliane Bettencourt. This work was granted by the Franco-Lao program, 'Biology, Ecology and Genetics of *Laonastes aenigmamus* living fossil in the Lao PDR', in Cooperation with the Lao PDR Ministry of Agriculture (PICS CNRS EDD 4166D). We want to thank Dr Bounthong Bouahom, Director of the National, Agricultural and Research Institute (NAFRI), for his gracious support and interest for our investigation efforts.

References

Baylac M (2012) Rmorph: a 'R' geometric multivariate morphometrics library.

Becht G (1953) Comparative biologic-anatomical researches on mastication in some mammals, I and II. *Proc Koninklijke Nederlandse Akademie van Wetenschappen* **56**, 508–527.

Carrier DR (1983) Postnatal ontogeny of the musculo-skeletal system in the black-tailed jack rabbit (*Lepus californicus*). *J Zool (Lond)* **201**, 27–55.

Carrier DR (1995) Ontogeny of jumping performance in the black tailed jack rabbit (*Lepus californicus*). *Zoology* **94**, 309–313.

Carrier DR (1996) Ontogenetic limits on locomotor performance. *Physiol Zool* **69**, 467–488.

Cox PG, Jeffery N (2011) Reviewing the morphology of the jaw-closing musculature in squirrels, rats and guinea pigs with contrast-enhanced microCT. *Anat Rec* **294**, 915–928.

Dawson MR, Marivaux L, Li C, et al. (2006) *Laonastes aenigmamus* and the 'Lazarus effect' in recent mammals. *Science* **311**, 1456–1458.

De Beer GR (1937) *The Development of the Vertebrate Skull*. Oxford: Clarendon Press.

Druzinsky RE (2010a) Functional anatomy of incisal biting in *Aplodontia rufa* and sciuromorph rodents – part 1: masticatory muscles, skull shape and digging. *Cells Tiss Org* **191**, 510–522.

Druzinsky RE (2010b) Functional anatomy of incisal biting in *Aplodontia rufa* and sciuromorph rodents – Part 2: sciuromorphy is efficacious for production of force at the incisors. *Cells Tiss Org* **192**, 50–63.

Flores DA, Abdala F, Giannini N (2010) Cranial ontogeny of *Caluromys philander* (Didelphidae: Caluromyinae): a qualitative and quantitative approach. *J Mamm* **91**, 539–550.

Genbrugge A, Heyde A-S, Adriaens D, et al. (2011) Ontogeny of the cranial skeleton in a Darwin's finch (*Geospiza fortis*). *J Anat* **219**, 115–131.

Goswami A (2007) Modularity and sequence heterochrony in the mammalian skull. *Evol Devel* **9**, 291–299.

Gunz P, Mitteroecker P, Bookstein FL (2005) Semi-landmarks in three dimensions. In: *Modern Morphometrics in Physical Anthropology*. (ed. Slice D), pp. 73–98. New York: Plenum Press.

Hautier L (2010) Masticatory muscle architecture in the gundi *Ctenodactylus vali* (Mammalia, Rodentia). *Mammalia* **74**, 153–152.

Hautier L, Saksiri S (2009) Masticatory muscles architecture in the Laotian rock rat *Laonastes aenigmamus* (Rodentia, Diatomyidae): new insights into the evolution of hystricognathy. *J Anat* **215**, 401–410.

Hautier L, Lebrun R, Saksiri S, et al. (2011a) Hystricognathy vs. sciurognathy in the rodent jaw: a new morphometric assessment of hystricognathy applied to living fossil *Laonastes* (Rodentia, Diatomyidae). *PLoS ONE*, **6**, e18698. doi:10.1371/journal.pone.0018698.

Hautier L, Weisbecker V, Goswami A, et al. (2011b) Skeletal ossification and sequence heterochrony in xenarthran evolution. *Evol Devel* **13**, 460–476.

Herrel A, Gibb AC (2006) Ontogeny of performance in vertebrates. *Physiol Biochem Zool* **79**, 1–6.

Herrel A, Holanova V (2008) Cranial morphology and bite force in *Chamaeleolis* lizards, adaptations to molluscivory? *Zoology* **111**, 467–475.

Herrel A, Van Wassenbergh S, Wouters S, et al. (2005) A functional morphological approach to the scaling of the feeding system in the African catfish, *Clarias gariepinus*. *J Exp Biol* **208**, 2091–2102.

Herrel A, De Smet A, Aguirre LF, et al. (2008) Morphological and mechanical determinants of bite force in bats: do muscles matter? *J Exp Biol* **211**, 86–91.

Huchon D, Chevret P, Jordan U, et al. (2007) Multiple molecular evidences for a living mammalian fossil. *Proc Natl Acad Sci USA* **104**, 7495–7499.

Hughes PCR, Tanner JM, Williams JPG (1978) A longitudinal radiographic study of the growth of the rat skull. *J Anat* **127**, 83–91.

Jenkins PD, Kilpatrick CW, Robinson MF, et al. (2005) Morphological and molecular investigations of a new family, genus and species of rodent (Mammalia: Rodentia: Hystricognatha) from Lao PDR. *Syst Biodiv* **2**, 419–454.

La Croix S, Zelditch M, Shivik JA, et al. (2011) Ontogeny of feeding performance and biomechanics in coyotes. *J Zool* **285**, 301–315.

Maier W, Klingler P, Ruf I (2003) Ontogeny of the medial masseter muscle, pseudo-myomorphy, and the systematic position of the Gliridae. *J Mammal Evol* **9**, 253–269.

Méndez J, Keys A (1960) Density and composition of mammalian muscle. *Metabolism* **9**, 184–188.

Offermans M, De Vree F (1989) Morphology of the masticatory apparatus in the springhare, *Pedetes capensis*. *J Mammal* **70**, 701–711.

Onoda Y, Westoby M, Adler PB, et al. (2011) Global patterns of leaf mechanical properties. *Ecol Lett* **14**, 301–312.

R Development Core Team (2010) *R: A Language and Environment for Statistical Computing*. Vienna, Austria: R Foundation for Statistical Computing.

Rohlf FJ, Slice DE (1990) Extensions of the procrustes method for the optimal superimposition of landmarks. *Syst Zool* **39**, 40–59.

Sánchez-Villagra MR, Goswami A, Weisbecker V, et al. (2008) Conserved relative timing of cranial ossification patterns in early mammalian evolution. *Evol Devel* **10**, 519–530.

Schumacher GH (1961) *Funktionelle morphologie der kaumuskulatur*. Jena: Gustav Fisher.

Scopin AE, Saveljev AP, Suntsova NA, et al. (2011) Digestive system of the Laotian rock rat *Laonastes aenigmamus* (Rodentia: diatomyidae) from the evolutionary viewpoint. *Proc Zool Inst RAS* **315**, 3–18.

Smith KK (1994) Development of craniofacial musculature in *Monodelphis domestica* (Marsupialia, Didelphidae). *J Morphol* **222**, 149–173.

Strong RM (1926) The order, time and rate of ossification of the albino rat (*Mus norvegicus albinus*) skeleton. *Am J Anat* **36**, 313–355.

Tanner JB, Zelditch ML, Lundrigan BL, et al. (2010) Ontogenetic change in skull morphology and mechanical advantage in the Spotted Hyena (*Crocuta crocuta*). *J Morphol* **271**, 353–365.

Vlassenbroeck J, Dierick M, Masschaele B, et al. (2007) Software tools for quantification of X-ray microtomography at the UGCT. *Nucl Instr Meth Phys Res A* **580**, 442–445.

Weijs WA (1973) Morphology of the muscles of mastication in the albino rat, *Rattus norvegicus* (Berkenhout, 1769). *Acta Morphol Neerl Scand* **11**, 321–340.

Wiley DF, Amenta N, Alcantara DA, et al. (2005) Evolutionary morphing. In: Proceedings of IEEE Visualization 2005 (VIS'05), 23–28 October 2005, Minneapolis, MN, USA.

Wilson D, Reeder D (2005) *Mammal Species of the World*. Baltimore: Johns Hopkins University Press.

Wilson LAB, Sanchez-Villagra MR (2009) Heterochrony and patterns of cranial suture closure in hystricognath rodents. *J Anat* **214**, 339–354.

Woods CA (1972) Comparative mycology of jaw, hyoid, and pectoral appendicular regions of new and old world hystricomorph rodents. *Bull Am Mus Nat Hist* **147**, 115–198.

Woods CA, Hermanson JW (1985) Myology of hystricognath rodents: an analysis of form, function and phylogeny. In *Evolutionary Relationships among Rodents, a Multidisciplinary Analysis* (eds Luckett WP, Hartenberger J-L). pp. 515–548. New York: Plenum Press.

Wright BW, Prodhan R, Wright K, et al. (2008) Mandibular morphology as it relates to ingestive and digestive folivory in *Trachypithecus* and *Pygathrix*. *Vietnamese J Primatol* **2**, 25–32.

Wyckmans M, Van Wassenbergh S, Adriaens D, et al. (2007) Size-related changes in cranial morphology affect diet in the catfish *Clariallabes longicauda*. *Biol J Linn Soc* **92**, 323–334.

Zelditch M (2004) *Geometric Morphometrics for Biologists: A Primer*. Amsterdam: Elsevier Academic Press.